Multiple configurations of *N*-methylpyrrole binding on Si(111)-7×7

Feng Tao, Ze Liang Yuan, Xian Feng Chen, Ming Hua Qiao, Zhong Hai Wang, Yu Jing Dai, Hai Gou Huang, Yong Cao, and Guo Qin Xu*

Department of Chemistry, National University of Singapore, 10 Kent Ridge, Singapore, 119260

(Received 24 June 2002; published 6 June 2003)

The adsorption configurations of *N*-methylpyrrole on Si(111)-7×7 were investigated using high-resolution electron energy-loss spectroscopy, x-ray photoelectron spectroscopy (XPS), scanning tunneling microscopy (STM), and density function theory calculations. Compared to physisorbed *N*-methylpyrrole, chemisorbed molecules present a different vibrational feature at 2886 cm^{-1} attributable to $\nu[(Si)C^{sp^3}\text{-}H]$ in addition to the vibrational features of $(sp^2)C^{\alpha}$-H (3106 cm^{-1}), $(sp^2)C^{\beta}$-H (3050 cm^{-1}), and C—H of CH_3 (2944 cm^{-1}) stretching modes, demonstrating the direct interaction between C═C bonds and Si(111)-7×7. The major change of *N* 1*s* XPS spectrum of *N*-methylpyrrole upon chemisorption strongly suggests the coexistence of two chemisorption states, further confirmed in the strong dependence of STM image features on the sample bias together with statistical analysis. The concurrent occurrence of [4+2] and [2+2] cycloadditions is proposed to account for these two adsorption configurations of *N*-methylpyrrole on Si(111)-7×7.

DOI: 10.1103/PhysRevB.67.245406 PACS number(s): 68.43.Fg, 82.65.+r

I. INTRODUCTION

The study of semiconductor surface electronic structures has been one of the most active areas of surface science. Although the correlation of surface electronic structures with physical properties was well understood, its relation with surface chemical reactivity is still to be established.[1,2] This knowledge, however, is scientifically and technologically important in developing new semiconductor-based devices and designing molecular electronics. Recent studies demonstrated that Si(111)-7×7 can act as a template to bind covalently with some unsaturated organic molecules due to its suitable spatial arrangement of surface dangling bonds and unique distribution of electronic density on surface Si atoms.[3–6]

The Si(111)-7×7 surface structure is schematically shown in Fig. 1, based on the Dimer-Adatom-Stacking (DAS) faulted mode.[7,8] Starting with three-coordinated Si atoms in every bulk-truncated unit cell of a (7×7) dimension, the surface undergoes a complicated reconstruction, decreasing the number of dangling bonds in a unit cell from 49 to 19. These dangling bonds consist of 6 ''rest atoms,'' 12 ''adatoms,'' and 1 ''corner hole.'' In fact, the most complicated and important is the redistribution of 19 electrons accompanying the spatial reconstruction of surface Si atoms. Upon reconstruction, each rest atom has a charge of −1, but $+\frac{7}{12}$ for every adatom. The great difference in electron density and the spatial separation (~4.5 Å) between the adjacent adatom and rest atom make them an efficient *di*-radical in the covalent attachment of unsaturated organic molecules.[3–6]

Earlier studies in this area mainly focused on the binding of ethylene,[9,10] acetylene,[11–13] benzene,[14,15] and chlorobenzene.[16,17] Experimental results and theoretical calculations suggest the [2+2]-like cycloaddition mechanism[9] for molecules containing one C═C bond[10–13] and [4+2]-like cycloaddition pathway[14] for dienelike molecules.[15–17] Recently, the attention is being directed towards the reactivity and selectivity of five-membered heterocyclic aromatic molecules on Si(111)-7×7. We showed that the radical nature of the electron-deficient Si dangling bonds plays an essential role in the [4+2]-like cycloaddition of thiophene on the Si(111)-7×7 surface.[4] These studies demonstrated that the Si dangling bonds can be alternatively viewed as reactive ''free radicals'' involving in surface-attachment reactions. Most recently, we have revealed the dimerization of adsorbed furan on the Si(111)-7×7 surface.[5] This facile reaction is attributed to the recombination of pairs of adjacent *mono-σ* bonded complexes at low temperature, displaying the formation of new Si—C and C—C covalent bonds. For pyrrole on Si(111)-7×7,[18] however, the adsorption behavior is distinctly different from thiophene and furan, possibly due to the presence of H—N bond in the molecule. Our studies showed that pyrrole adsorbs on Si(111)-7×7 through the dissociation of N—H bond, forming pyrrolyl-covered Si surfaces. The aromatic ring retained at the organic/silicon interface may be used as a

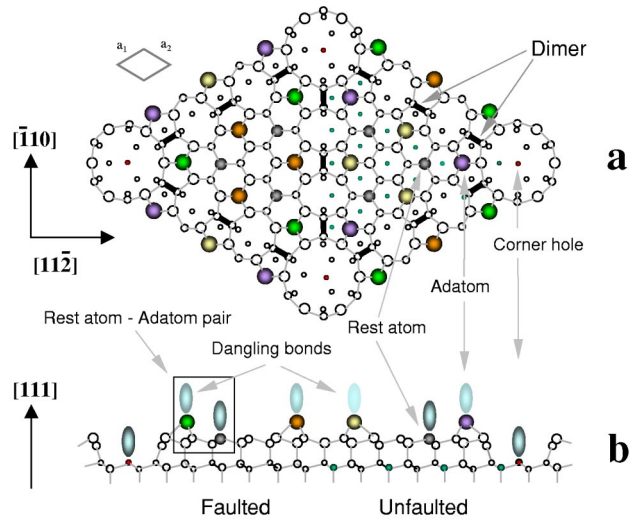

FIG. 1. (Color online) The top (a) and side (b) views of the detailed three-dimensional structure of an Si(111)-7×7 unit cell on the basis of the dimer-adatom-stacking (DAS) faulted 7×7 model.

precursor for further modification of Si surfaces or materials syntheses through typical reaction of pyrrolyl including cycloaddition, α-H substitution reaction and polymerization.

N-methylpyrrole, a substituted five-membered heterocyclic aromatics is expected to present binding modes different from pyrrole on Si(111)-7×7. Replacing the H-(*N*) of pyrrole by CH_3-(N) may open the [4+2] or/and [2+2] cycloadditions for *N*-methylpyrrole on the surface, providing the chemical flexibility in the selection of reaction pathway. Our investigation was carried out using a combination of high-resolution electron energy-loss spectroscopy (HREELS), x-ray photoelectron spectroscopy (XPS), scanning tunneling microscopy (STM), and density-functional theory (DFT) calculations. We found that *N*-methylpyrrole is attached covalently to the silicon surface with two concurrent binding configurations corresponding to [4+2] and [2+2] cycloadditions with a ratio of ~60%:40%.

II. EXPERIMENT

The experiments were performed in three separate UHV chambers. All of them have a base pressure of $<2\times10^{-10}$ Torr, achieved with turbomolecular and sputtered-ion pumps. The first UHV chamber was equipped with an x-ray gun (both Mg and Al anodes) and hemispherical electron energy analyzer (CLAM 2, VG) for XPS. The HREELS chamber mainly consists of a high-resolution electron energy-loss spectrometer (HREELS, LK-2000-14R) and a quadruple mass spectrometer (UTI-100) for gas analysis. The STM system includes a sample preparation chamber and the Omicron VT STM chamber.

For HREELS experiments, the electron beam with an energy of 5.0 eV impinges on Si(111)-7×7 at an incident angle of 60° with a resolution of 5–6 meV [full width at half maximum (FWHM), 40–50 cm^{-1}]. XPS spectra were acquired using Mg $K\alpha$ radiation ($h\nu=1253.6$ eV) and a 20-eV pass energy. For XPS, the binging energy (BE) scale is referenced to the peak maximum of the Si $2p$ line (99.3 eV calibrated for Au $4f_{7/2}$) (Ref. 19) of Si(111)-7×7 with a FWHM of less than 1.2 eV. The constant current topographs (CCT's) of the clean and *N*-methylpyrrole-exposed Si(111)-7×7 were obtained with a sample bias of $V_s=1-3$ V and a tunneling current of $I_t=0.15-0.2$ nA at 300 K.

For HREELS and XPS experiments, the samples with a dimension of $8\times18\times0.35$ mm^3 ($3\times8\times0.35$ mm^3 for STM experiments) were cut from *n*-type Si(111) wafers (*Phosphors* doped, with a resistivity of 1–30 Ω cm, 99.999%, Goodfellow). A Ta-sheet heater (0.025 mm thick, Goodfellow) was sandwiched tightly between two Si(111) crystals held together by two Ta clips. A 0.003 in. W-5% Re/W-26%Re thermocouple was attached to the center of one of silicon samples using a high-temperature ceramic adhesive (Aremco 516) for temperature measurement and control. Uniform heating of the samples was achieved by passing current through the Ta heater. This sample-mounting configuration allows us to resistively heat the samples to 1400 K and conductively cool them to 110 K using liquid nitrogen. The temperature distribution on the samples is within ±10 K at 1000 K, determined using a pyrometer ($\varepsilon=0.74$, TR-630, Minolta).

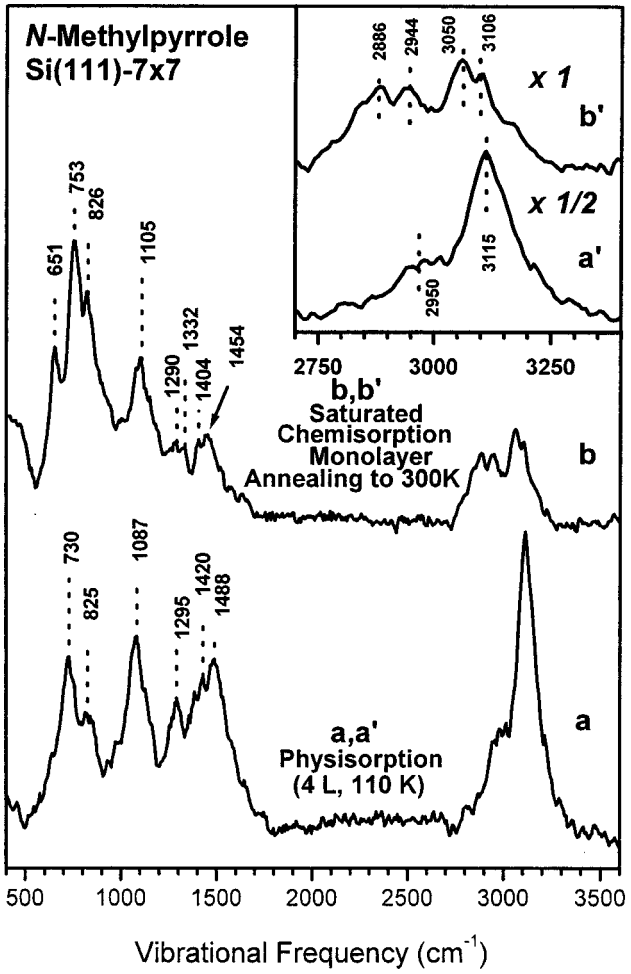

FIG. 2. HREELS spectra of physisorbed and saturated chemisorption *N*-methylpyrrole on Si(111)-7×7. $E_p=5.0$ eV, specular geometry. The chemisorption monolayer was prepared by annealing the multilayer *N*-methylpyrrole-covered surface to 300 K, desorbing physisorbed molecules.

The Si(111) sample was cleaned by repeated ion sputtering-annealing cycles (500-eV Ar^+ bombardment for 30 min with an ion current density of ~5 $\mu A\,cm^{-2}$ and subsequent annealing at 1250 K for 20 min). The surface cleanliness was routinely monitored using XPS and HREELS. The (7×7) reconstruction formed after the final annealing was confirmed using STM. *N*-methylpyrrole (Aldrich, 99.5+%) was purified by freeze-pump-thaw cycles and dosed onto Si(111)-7×7 through a variable leaking valve without the calibration of ion gauge sensitivity.

III. RESULTS AND DISCUSSION

A. High-resolution electron energy-loss spectroscopy

Figure 2 shows the high-resolution electron energy-loss spectroscopy after *N*-methylpyrrole adsorption on Si(111)-7×7. Figure 2(a) is the vibrational features of physisorbed multilayer *N*-methylpyrrole prepared by exposing

TABLE I. Assignments of the vibrational frequencies for physisorbed and chemisorbed *N*-methylpyrrole on Si(111)-7×7 (unit in cm^{-1}).

Vibrational mode[a]	Gaseous pyrrole[a]	Physisorbed *N*-methylpyrrole	Chemisorbed *N*-methylpyrrole
ν(Si—C)			651
γ(CH)(B_2)	768	730	753
δ(ring)(B_1)	869	825	826
δ(CH)(A_1)	1047	1087	1105
δ(CH)(B_1)	1076		
	1290		1290
	1380	1295	1332
ν(ring)(A_1)	1418	1420	1404
ν(ring)(B_1)	1466	1488	1454
	1531		
$\nu(C^{sp3}H)(A_1)$ for Si—CH			2886
$\nu(C^{sp3}H)(A_1)$ for N—CH_3		2950	2944
$\nu(C^{sp2}H)(A_1)$	3133	3115	3050, 3106
ν(NH)(A_1)	3400		

[a]References 20 and 21.

N-methylpyrrole vapor onto Si(111)-7×7 at 110 K. Figure 2(b) is the vibrational signatures of saturated chemisorption *N*-methylpyrrole on Si(111)-7×7. The vibrational frequencies of physisorbed *N*-methylpyrrole and chemisorbed molecules are assigned according to the relevant vibrational modes of gaseous phase pyrrole[20] (Table I) due to the lack of detailed vibrational assignments of free *N*-methylpyrrole. The vibrational signatures of physisorbed molecules are well in line with the infrared spectrum of liquid phase *N*-methylpyrrole[21] although the detailed assignments are not available.

The features of chemisorbed *N*-methylpyrrole [Fig. 2(b)], however, are different from the above-mentioned physisorbed molecules [Fig. 2(a)]. The major difference lies in the C—H stretching region that is enlarged and clearly presented in the inset of Fig. 2. In the spectrum of physisorbed *N*-methylpyrrole [Fig. 2(a')], the broad feature around 3115 cm^{-1} is associated with $(sp^2)C^{\alpha}$—H and $(sp^2)C^{\beta}$—H and a shoulder at ~2950 cm^{-1} ascribed to (sp^3)C—H of CH_3 group. Compared to physisorbed molecules, the vibrational feature of chemisorbed molecules [Fig. 2(b')] presents a new peak appears at 2886 cm^{-1}, possibly ascribed to $(Si)(sp^3)C^{\alpha}$—H and $(Si)(sp^3)C^{\beta}$—H stretching modes. The fact of observing two resolvable peaks at ~3106 and ~3050 cm^{-1}, respectively, attributable to $(sp^2)C^{\alpha}$—H and $(sp^2)C^{\beta}$—H,[20,21] shows that only a portion of C^{α} and C^{β} atoms in the molecule is rehybridized from sp^2 into sp^3 upon chemisorption. Another solid evidence for the direct interaction of (sp^2)C atoms with Si surface dangling bonds is the appearance of a vibrational feature at 651 cm^{-1} assigned to Si—C stretching mode.[22] Moreover, the absence of the ν(Si—H) intensity at ~2000–2100 cm^{-1} in the present case readily excludes the formation of the σ-bonded species involving C—H bond scission and Si—H bond formation.[23]

A schematic presentation of [4+2]- and [2+2]-like cycloaddtion reactions is shown in Fig. 3. The fact that only a portion of C^{α} and C^{β} atoms of the molecule is directly involved in the covalent bonding with Si surface dangling bonds strongly suggests the involvement of the [2+2]-like cycloaddition between one of the two C^{α}=C^{β} bonds of the molecule and adjacent adatom-rest atom pair in chemisorption. Our HREELS result excludes the possibility of [4+2] cycloadduct as the sole product because the [4+2]-like

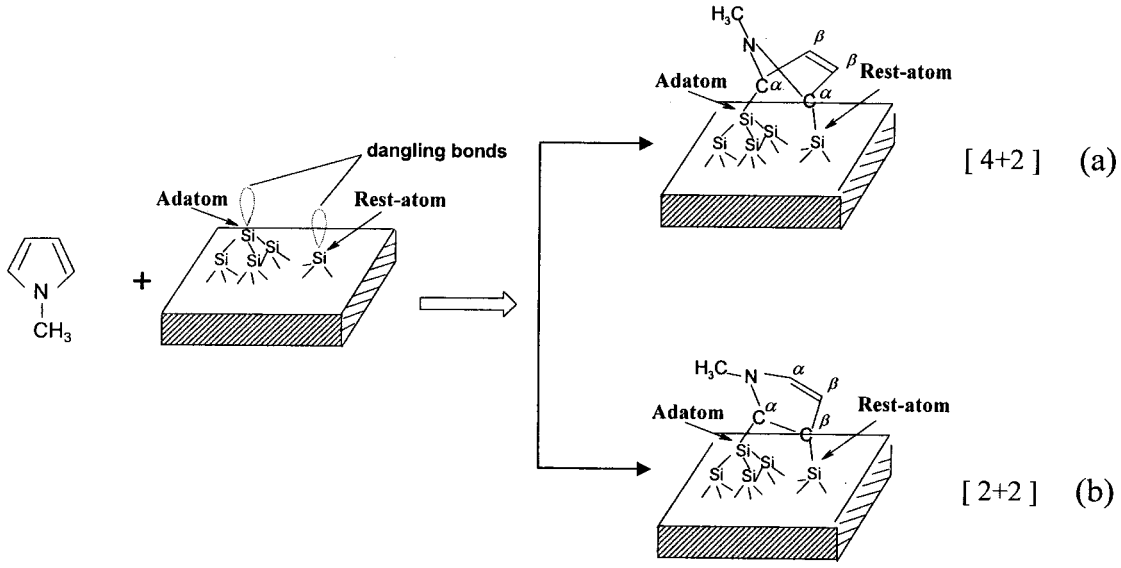

FIG. 3. Schematic presentation of possible adsorption products of *N*-methylpyrrole on Si(111)-7×7 through [4+2] and [2+2] cycloadditions.

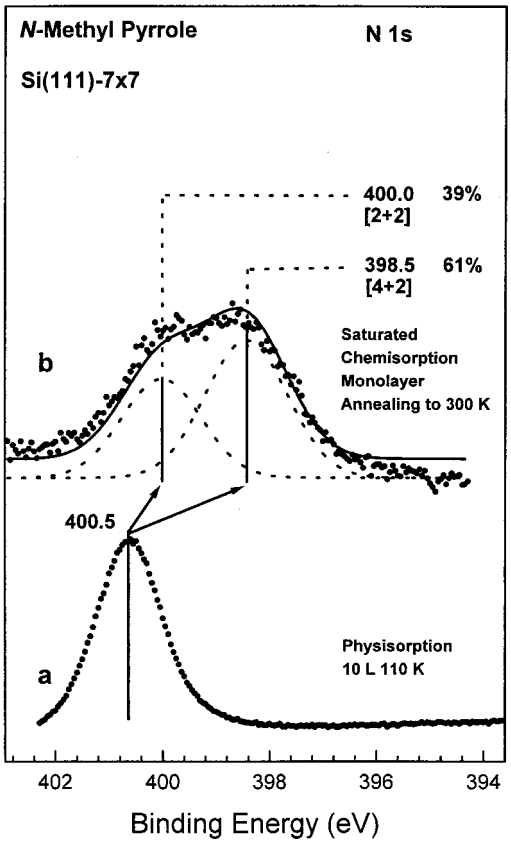

FIG. 4. *N* 1*s* spectra of physisorbed and saturated chemisorption *N*-methylpyrrole on Si(111)-7×7 together with the fitting results.

addition between two C^{α} atoms and adatom-rest atom pair results in only C^{β} atoms with sp^2 hybridization. However, the concurrent occurrence of these two reactions cannot be ruled out based on the vibrational studies. To further resolve these possibilities, the chemical shifts of *N* 1*s* core level upon chemisorption were measured and found to be very helpful.

B. X-ray photoelectron spectroscopy

Figure 4 shows the *N* 1*s* photoemission spectra of physisorbed *N*-methylpyrrole and saturated chemisorption molecules together with the deconvolution results. *N* 1*s* photoemission spectrum of physisorbed molecules contains a symmetric peak at 400.5 eV with a typical FWHM (~1.2 eV) under our XPS resolution. This binding energy is consistent with the value (400.3 eV) of physisorbed pyrrole on Si(100).[24] The slight difference of 0.2 eV is possibly resulted from the different electronic affinity between—the CH_3 group of *N*-methylpyrrole and the H atom of pyrrole. Compared to Fig. 4(a), however, significant changes can be found in the *N* 1*s* spectrum of saturated chemisorption molecules [Fig. 4(b)]. The *N* 1*s* feature is significantly broadened with a FWHM of 3.0 eV and an asymmetric flat-top shape which can be fitted into two peaks centered at 400.0 and 398.5 eV. The area ratio for these two peaks is 39%:61%, approximately 2:3. The coexistence of two *N* 1*s* peaks with a large separation of 1.5 eV indicates that there are two chemisorption states with different electronic environments.

Although the nitrogen atom with lone pair electrons possibly acts as an electron donor to Si surface dangling bonds, the down-shift of *N* 1*s* core level of chemisorbed molecules compared to physisorbed *N*-methylpyrrole does not support such lone pair electrons transferring from N atom to the silicon surface. Thus the possibility of forming dative bond can be readily ruled out. This is understandable since the lone pair electrons are delocalized in the large aromatic system formed together with the four π electrons of four C (sp^2) atoms. For this reason, in pyrrole/Si(100) (Refs. 24 and 25) and pyrrole/Si(111)-7×7 (Ref. 18) and *N*-methylpyrrole/Si(100) (Ref. 26) systems, dative bond is not observed.

In the [4+2] cycloaddition reaction [Fig. 3(a)], the two C^{α} atoms rehybridizing from sp^2 to sp^3 are bonded to two Si atoms with a much lower electronegativity (Pauling electronegativity=1.90), enhancing the charge transfer from C^{α} to the N atom. In addition, compared to physisorbed *N*-methylpyrrole, the aromaticity of the ring is broken and the lone-pair electrons are totally localized on the N atom. Thus a lower *N* 1*s* BE at 398.5 eV upon chemisorption is attributable to the [4+2]-like cycloadduct.

In the [2+2] addition product [Fig. 3(b)], however, only one C^{α} rehybridizes into C^{sp3} and directly bonds to Si atom, increasing the electron density on the N atom through the $(sp^3)C^{\alpha}$—N bond. The other C^{α} atom remains its sp^2 hybridization upon chemisorption. On the other hand, in this skeleton —$C^{\beta}H{=}C^{\alpha}H$—$N(CH_3)$—$C^{\alpha}H(Si)$—$C^{\beta}H(Si)$—, there is a hyperconjugation effect between the $\pi(C^{\alpha}{=}C^{\beta})$ and the lone electron pair of neighboring N atom, resulting in partial electron density transferring from the N atom to C^{α} (sp^2). The combined effects produce a slight down-shift (0.5 eV) of *N* 1*s* core level upon chemisorption. Based on the above discussion, it is reasonable to assign the *N* 1*s* peak at 400.0 eV to the [2+2]-like cycloadduct. Thus our XPS studies demonstrate the concurrent occurrence of the [2+2] and [4+2] addition reactions for *N*-methylpyrrole chemisorption on Si(111)-7×7.

C. Scanning tunneling microscopy

To further elucidate the nature of *N*-methylpyrrole chemisorbed on Si(111)-7×7, STM was employed to investigate its site selectivity. Figure 5(a) is the STM constant current topograph (CCT) of a clean Si(111)-7×7 surface with a defect density of <1%, estimated by counting an area containing about one thousand adatoms (not shown). Figure 5(b) is the STM image obtained after *N*-methylpyrrole adsorption in the same region as that of Fig. 5(a). The defects marked with arrow are used to identify the location of all the other adatoms before and after chemisorption. Compared to the clean Si(111)-7×7 surface [Fig. 5(a)], the protrusions of one center adatom and three-corner adatoms in regions 1 and 2 (labeled with yellow cycles in Fig. 5), respectively, disappear upon chemisorption. In addition, one-center adatoms and one corner adatom in regions 1 and 2 (marked with yellow squares) are *dimmer* after adsorption reaction. The darkened or dim adatoms in Fig. 5(b) indicate the disappear-

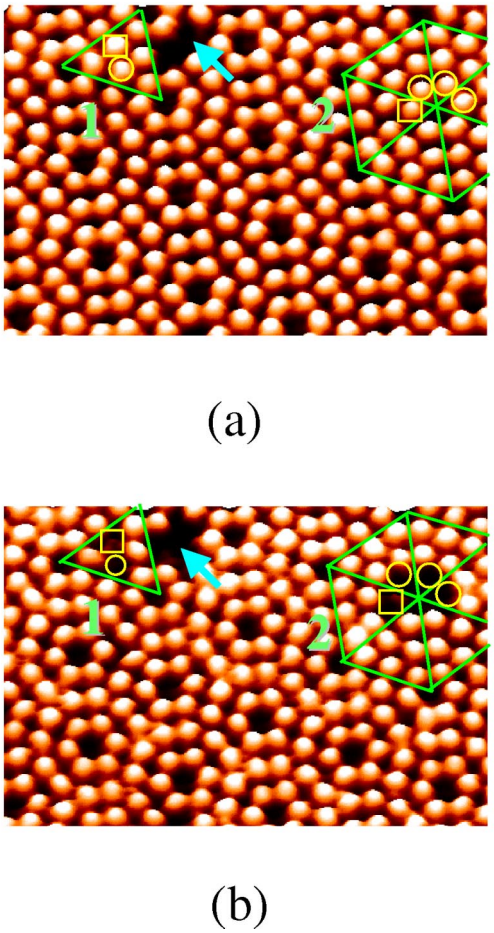

FIG. 5. (Color online) Constant-current-topograph (CCT) images (sample bias of +1.5 V) of (a) clean and (b) *in situ* *N*-methylpyrrole-exposed Si(111)-7×7 with a low exposure of 0.10 L.

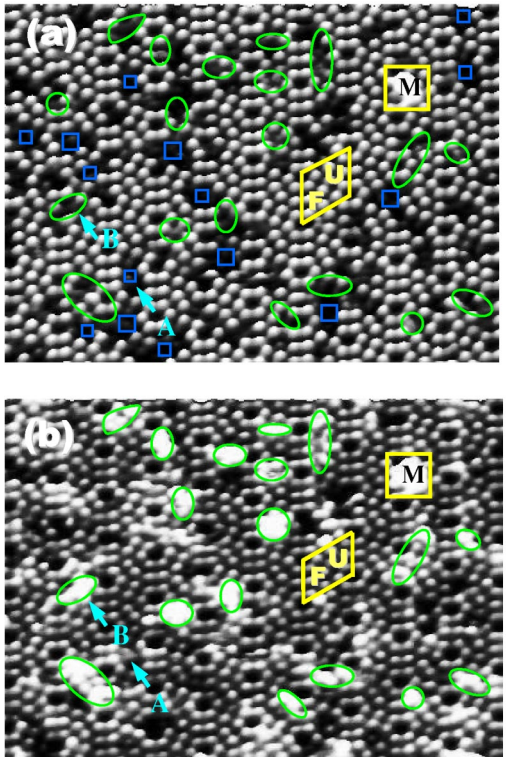

FIG. 6. (Color online) Constant-current-topograph (CCT) images of Si(111)-7×7 exposed with 6-L *N*-methylpyrrole at the sample-bias of +1.5 V (a) and +3.0 V (b). M is the defects used to locate all the other adatoms upon changing sample-bias.

ance of the dangling-bond surface states and the elimination of electron density at these sites due to the chemisorption. The formation of darkened or dim sites, whose number increases with exposure, was also observed for the chemisorption of other small molecules on Si(111)-7×7, including C_2H_2,[27] C_2H_4,[28] C_4H_4S,[4,29] C_6H_6,[30] C_6H_5Cl,[31,32] C_6H_5CN,[33] NH_3.[34] In all these systems, the darkening of adatoms in the STM images was attributed to the consumption of dangling bonds of adatoms to form new surface-adsorbate bonds.

The images in Figs. 6(a) and 6(b) were taken at sample biases of +1.5 and +3.0 V, respectively, for Si(111)-7×7 exposed with 6 L *N*-methylpyrrole at 300 K. Surprisingly, the image features vary significantly with bias. At the sample bias of +1.5 V [Fig. 6(a)], some adsorbed molecules are clearly presented as darkened sites (chemisorbed state A, around solid blue squares) ascribed to the disappearance of the dangling bonds of these adatoms. In addition, a more careful observation seemingly suggests another possible adsorption state (B), labeled with green elliptic lines, appearing as slightly *dimmer* protrusions compared to unreacted adatoms in Fig. 6(a). Notably, the difference in brightness between adsorption state B and unreacted adatoms is small. In order to confirm the existence of adsorption state B, sample-bias evolution technique was commanded.

At the sample bias of +3.0 V [Fig. 6(b)], the feature corresponding to possible adsorption state B appears as much brighter protrusions compared to the unpassivated adatoms. The adsorption state A [the darkened sites labeled with blue solid squares in Fig. 6(a)] also brightens and displays as protrusions similar to those of unreacted adatoms. The distinctly different brightnesses of chemisorption state A at sample biases of 1.5 and 3.0 V may suggest that some unoccupied molecular orbitals at higher energy levels are readily accessible to the tunneling process. Similarly, the strong dependence of image features of chemisorption state B on the sample bias possibly indicates that even greater contribution of unoccupied molecular orbitals at high sample bias.

Chemisorption state A appears as darkened sites at low bias [Fig. 6(a)] and state B is characterized as much brighter protrusions than state A at high bias [Fig. 6(b)]. By making use of these differences, statistical counting for the STM images of *N*-methylpyrrole-saturated Si(111)-7×7 surface obtained at +1.5 and +3.0 V reveals that the ratio of reacted adatoms corresponding to chemisorption states A and B are 42%:58%, close to the ratio (39%:61%) from the XPS experiments. Therefore the chemisorption states A and B resolved by STM images may possibly be assigned to the [2+2] and [4+2] cycloaddition products, respectively. A careful examination shows that the green circles contain a variable number of reacted adatoms aligned in rows [Fig.

TABLE II. Statistic counting of reactive adatom for *N*-methylpyrrole chemisorbed on Si(111)-7×7 at 300 K.

		Faulted halves			Unfaulted halves		
Exposure (L)	Absolute coverage	Center adatoms	Corner adatoms	Sum of adatom	Center adatoms	Corner adatoms	Sum of adatom
0.5	9.5%	62	28	90	45	19	64
1.5	14.8%	138	54	192	75	40	115
2.5	17%	146	65	211	102	47	149

6(a)]. Although these sites are brightened at a bias of 3.0 V, some variation in their intensity can be noticed [Fig. 6(b)]. These results imply the possible existence of attractive interaction between the [4+2] cycloadducts.

Statistical counting of STM images can also provide information on the site selectivity for chemisorbed *N*-methylpyrrole at atomic resolution. The inspection of different exposures of *N*-methylpyrrole (Table II) manifests the preferential adsorption on the center adatom sites of faulted halves. The center adatoms are found to have a higher reactivity than corner adatoms in both faulted and unfaulted subunits. Besides, the adatoms in faulted subunits react preferentially over those in unfaulted subunits with a ratio of ~3:2 at low exposures as listed in Table II.

The higher selectivity of *N*-methylpyrrole on the faulted half of a Si(111)-7×7 unit cell can be understood by considering the higher electrophilicity of faulted subunits.[27] On the other hand, the DAS (7×7) model shows that reaction occurring at the corner adatom will strain two dimer bonds, while the reaction at the center adatom will encounter only one. Therefore a smaller strain induced by adsorbed *N*-methylpyrrole at a center-adatom site would result in a lower transition state, leading to a higher reaction rate at the center adatom sites.[35]

D. Theoretical calculations

The [4+2]-like cycloadduct is formed through a cycloaddition reaction between a conjugated diene and a ''dienophile,'' which in this case is the adjacent adatom-rest atom pair of Si(111)-7×7. It has a —(Si)C—C═C—C(Si)— structure. However, the [4+2] cycloaddition is not the only possible reaction pathway by which *N*-methylpyrrole can bind covalently to Si(111)-7×7. Similar to the surface reaction with ethylene[36] and acetylene,[28,37,38] conjugated 1,3-diene may also interact with the neighboring adatom–rest atom pair in a [2+2]-like fashion to form a product containing —(Si)C—C(Si)—C═C—

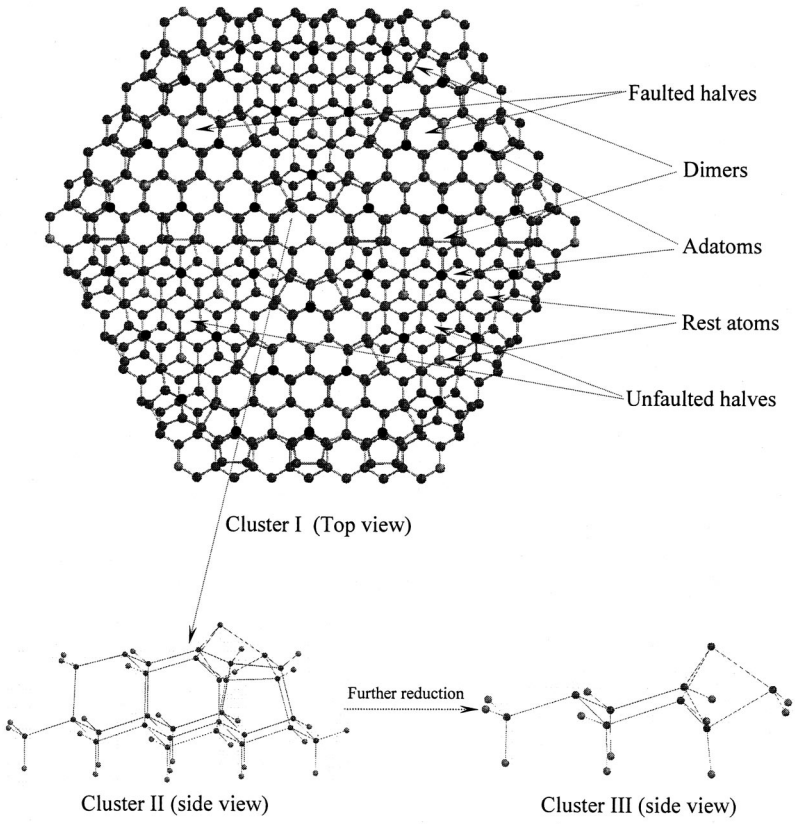

FIG. 7. A large cluster of the top five silicon layers constructed based on the DAS model to present three Si(111)-7×7 surface unit cells surrounding a corner hole. It (cluster I) has 973 atoms including the capping H atoms (not displayed for clarity). Clusters II ($Si_{30}H_{28}$) and III (Si_9H_{12}) are reduced from cluster I.

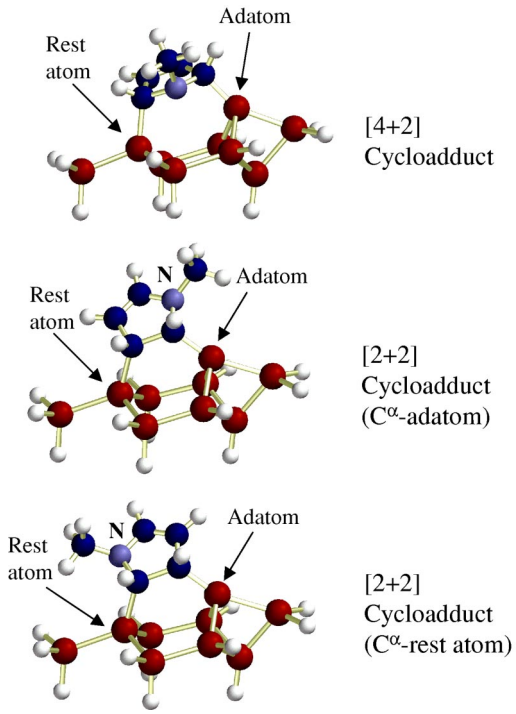

FIG. 8. (Color online) The optimized configurations corresponding to [4+2] cycloadduct and [2+2] addition products.

skeleton, involving only one $\pi_{C=C}$ bond. To further understand the reaction mechanisms of *N*-methylpyrrole on Si(111)-7×7, DFT calculations were carried out.

As shown in the left-bottom panel of Fig. 7, cluster II ($Si_{30}H_{28}$) was cut from the central part of MMFF94 (Ref. 39) optimized cluster I containing 973 atoms including the capping H atoms (the top panel of Fig. 7), where the precision of atomic positions suffers the least from boundary effects. Capping H atoms at the cluster boundaries are kept frozen. Silicon atoms in the bottom double layers are placed at bulk lattice positions prior to the geometry optimization process, with each Si—Si bond length set to 2.3517 Å and all bond angles adjusted to 109.4712°. Cluster III (Si_9H_{12}) was obtained from further reduction of cluster II. Similarly, all capping H atoms were frozen during geometry optimization. Clusters I, II, and III were constructed by us and successfully employed in predicting the adsorption energy of benzene on Si(111)-7×7.[15,40] Three modeling clusters for two configurations of [2+2]-like cycloadducts and one [4+2]-like addition product were constructed by the addition of C_5H_7N onto the mother cluster (cluster III of Fig. 7).

Adsorption energy, synonymous to formation heat, is quoted here as the difference *between* the total energy of the adsorbate/substrate complex *and* the total sum of the substrate and gaseous *N*-methylpyrrole. The adsorption energies

TABLE III. The adsorption energies of different adsorption configurations calculated by density-functional theory (pBP/DN**). All energies are in kcal mol^{-1}.

Calculation method	[4+2]-like cycloadduct	[2+2]-like cycloadduct (C^{α} bonded to adatom)	[2+2]-like cycloadduct (C^{β} bonded to adatom)
DFT (pBP/DN**)	38.0	23.0	23.1

of different products were calculated at the DFT theory level using perturbative Beck-Perdew functional (pBP86) in conjugation with a basis set of DN** (comparable 6-31 G**).[41] Geometric optimizations were conducted under SPARTAN default criteria before calculations. The optimized configurations corresponding to [4+2]-like and [2+2]-like cycloadducts are presented in Fig. 8. The calculated adsorption energies are tabulated in Table III. DFT calculation results show that the two possible [2+2]-like configurations have a similar adsorption energy, ~23 kcal mol^{-1}. However, this value is much smaller than that of the [4+2]-like addition product by ~15 kcal mol^{-1}. A similar trend is also predicted by the simple and low-cost semiempirical (PM3) calculation method. Although [4+2] cycloaddition is energetically preferred compared to [2+2] addition fashion, the coexistence of [4+2] and [2+2] cycloadducts from our experimental results suggests the surface reactions may be kinetically controlled. A ratio of 2:3 for [2+2] and [4+2] cycloaddition products implies a possible lower transition state for the [4+2] cycloaddition pathway due to the better geometric match between the ''diene'' of the molecule and the adjacent adatom–rest atom pair.

IV. SUMMARY

N-methylpyrrole is molecularly chemisorbed on Si(111)-7×7 at 300 K. The covalent binding of the molecule with the surface through cycloaddition reactions was clearly demonstrated in our HREELS studies. The *N* 1*s* core-level photoemission features of chemisorbed molecules suggest the coexistence of two chemisorption states corresponding to [4+2] and [2+2] cycloadducts, which was further confirmed in the STM studies. Statistical counting of STM images shows that the ratio between [4+2] and [2+2] cycloadducts is 42%:58%, close to the value (39%:61%) from the *N* 1*s* photoemission intensities. STM studies also reveal the preferential adsorption of *N*-methylpyrrole at center adatoms of faulted subunits. The chemisorption species formed on the surface may possibly be used as a precursor for further functionalization and modification of Si surfaces or as an intermediate for syntheses via the C=C bond.

*Corresponding author. Fax: (65) 6779 1691.

[1] R. A. Wolkow, Annu. Rev. Phys. Chem. **50**, 413 (1999).
[2] H. N. Waltenburg and J. T. Yates, Chem. Rev. (Washington, D.C.) **95**, 1589 (1995).
[3] R. J. Hamers, S. K. Coulter, M. D. Ellison, J. S. Hovis, D. F. Padowitz, M. P. Schwartz, C. M. Greenlief, and J. N. Russell, Jr., Acc. Chem. Res. **33**, 617 (2000).
[4] Y. Cao, K. S. Yong, Z. Q. Wang, W. S. Chin, Y. H. Lai, J. F. Deng,

and G. Q. Xu, J. Am. Chem. Soc. **122**, 1812 (2000).
[5] Y. Cao, Z. H. Wang, J. F. Deng, and G. Q. Xu, Angew. Chem., Int. Ed. Engl. **39**, 2740 (2000).
[6] F. Tao, Y. J. Dai, and G. Q. Xu, Phys. Rev. B **66**, 035420 (2002).
[7] K. Takayanagi, Y. Tanishiro, S. Takahashi, and M. Takahashi, Surf. Sci. **164**, 367 (1985).
[8] D. J. Chadi, Phys. Rev. Lett. **43**, 43 (1979).
[9] [2+2] cycloaddition refers to one C═C bond (2 C atoms) reacting with 2 Si-dangling bonds.
[10] M. Carbone, M. Zanoni, M. N. Piancastelli, G. Comtet, G. Dujardin, L. Hellner, and A. Mayner, J. Electron Spectrosc. Relat. Phenom. **76**, 271 (1995); M. Carbone, M. N. Piancastelli, M. P. Casaletto, R. Zanoni, G. Comtet, G. Dujardin, and J. L. Hellner, Phys. Rev. B **61**, 8531 (2000).
[11] F. Rochet, G. Dufour, P. Prieto, F. Sirotti, and F. C. Stedile, Phys. Rev. B **57**, 6738 (1998); F. Rochet, F. Jolly, G. Dufour, F. Sirotti, and J. L. Cantin, Phys. Rev. B **58**, 11 029 (1998).
[12] J. Yoshinobu, D. Fukushi, M. Uda, E. Nomura, and M. Aono, Phys. Rev. B **46**, 9520 (1992).
[13] B. Weiner, C. S. Carmer, and M. Frenklach, Phys. Rev. B **43**, 1678 (1991).
[14] [4+2] cycloaddition refers to the reaction between a conjugated diene (C═C—C═C, four C atoms) and two Si dangling bonds.
[15] Y. Cao, X. M. Wei, W. S. Chin, Y. H. Lai, J. F. Deng, S. L. Bernasek, and G. Q. Xu, J. Phys. Chem. B **103**, 5698 (1999).
[16] Y. Cao, J. F. Deng, and G. Q. Xu, J. Chem. Phys. **112**, 4759 (2000).
[17] X. M. Chen, Q. King, J. C. Polanyi, D. Rogers, and S. So, Surf. Sci. **340**, 224 (1995).
[18] Z. L. Yuan, X. F. Chen, Z. H. Wang, Y. Cao, and G. Q. Xu (unpublished).
[19] J. F. Moulder, W. F. Stickle, P. E. Sobol, and K. D. Bomben, *Handbook of X-Ray Photoelectron Spectroscopy* (Physical Electronics Division, Perkin-Elmer Corporation, MN, 1991).
[20] R. J. Lord and F. A. Miller, J. Chem. Phys. **10**, 328 (1942).
[21] C. J. Pouchert, *The Aldrich Library of FT-IR Spectra: Vapour Phase*, 3rd Ed. (Aldrich Chemical, Wisconsin, 1989).
[22] K. Hamaguchi, S. Machida, M. Nagao, F. Yasui, K. Mukai, Y. Yamashita, and J. Yoshinobu, J. Phys. Chem. B **105**, 3718 (2001).
[23] H. Wagner, R. Butz, U. Backes, and D. Bruchmann, Solid State Commun. **38**, 1155 (1981).
[24] M. H. Qiao, F. Tao, Y. Cao, Q. Liu, J. F. Deng, and G. Q. Xu (unpublished).
[25] X. Cao, S. K. Coulter, M. D. Ellison, H. Liu, J. Liu, and R. J. Hamers, J. Phys. Chem. B **105**, 3759 (2001).
[26] M. H. Qiao, F. Tao, Y. Cao, Q. Liu, J. F. Deng, and G. Q. Xu (unpublished).
[27] J. Yoshinobu, T. Tasuda, M. Onchi, and M. Nishijima, Chem. Phys. Lett. **130**, 170 (1986).
[28] J. Yoshinobu, D. Fukushi, M. Uda, E. Nomura, and M. Aono, Phys. Rev. B **46**, 9520 (1992).
[29] Y. Cao, K. S. Yong, Z. H. Wang, Y. H. Lai, J. F. Deng, and G. Q. Xu, J. Chem. Phys. **115**, 3287 (2001).
[30] T. Kawasaki, D. Sakai, H. Kishimoto, A. A. Akbar, T. Ogawa, and C. Oshima, Surf. Interface Anal. **31**, 126 (2001).
[31] P. H. Lu, J. C. Planyi, and D. Rogers, J. Chem. Phys. **111**, 9905 (1999).
[32] X. H. Chen, Q. Kong, J. C. Polanyi, D. Rogers, and S. So, Surf. Sci. **340**, 224 (1995).
[33] F. Tao, Z. H. Wang, X. F. Chen, and G. Q. Xu, Phys. Rev. B **165**, 11 531 (2002).
[34] Ph. Avouris and I. W. Lyo, Surf. Sci. **242**, 1 (1991).
[35] R. A. Wolkow and D. J. Moffatt, J. Chem. Phys. **103**, 10 696 (1995).
[36] M. Carbone, M. Zanoni, M. N. Piancastelli, G. Comtet, G. Dujardin, L. Hellner, and A. Mayner, J. Electron Spectrosc. Relat. Phenom. **76**, 271 (1995).
[37] F. Rochet, G. Dufour, P. Prieto, F. Sirotti, and F. C. Stedile, Phys. Rev. B **57**, 6738 (1998).
[38] M. N. Piancastell, N. Motta, A. Sgarlata, A. Balzarotti, and D. De. Crescenzi, Phys. Rev. B **48**, 17 892 (1993).
[39] T. A. Halgren, J. Comput. Chem. **17**, 490 (1996).
[40] Z. H. Wang, Y. Cao, and G. Q. Xu, Chem. Phys. Lett. **338**, 7 (2001).
[41] W. J. Hehre, J. Yu, P. E. Klunzinger, and L. Lou, *A Brief Guide to Molecular Mechanics and Quantum Chemical Calculation* (Wavefunction, Irvine, CA, 1998).